

The magnetic origin of multiferroic Y_2CoMnO_6

Ting Jia¹, Zhi Zeng^{1,2*}, X. G. Li³ and H. Q. Lin⁴

¹Key Laboratory of Materials Physics, Institute of Solid State Physics, Chinese Academy of Sciences, Hefei 230031, China

²Department of Physics, University of Science and Technology of China, Hefei, 230026, China

³Hefei National Laboratory for Physical Sciences at Microscale, Department of Physics, University of Science and Technology of China, Hefei 230026, China and

⁴Beijing Computational Science Research Center, Beijing 100084, China

(Dated: October 29, 2014)

It has been found experimentally that the ferroelectricity in Y_2CoMnO_6 is driven by a magnetic ordering of collinear up-up-down-down ($\uparrow\uparrow\downarrow\downarrow$). Here, the origin of the magnetism and thereby ferroelectricity is studied using first-principles calculations. We firstly confirm that the experimentally observed $\uparrow\uparrow\downarrow\downarrow$ antiferromagnetic structure is the ground state of Y_2CoMnO_6 . Additionally, both the Co^{2+} and Mn^{4+} are in the high-spin state. By analyzing the exchange coupling and corresponding pathways, we conclude that the $\uparrow\uparrow\downarrow\downarrow$ spin order in Y_2CoMnO_6 originates from a subtle competition between the ferromagnetic Co-O-Mn super-exchange and antiferromagnetic Co-Mn direct-exchange along c axis.

Magnetoelectric (ME) multiferroics with ferromagnetic and ferroelectric order in the same phase are interested due to their potential applications to memory and magnetic storage devices[1, 2]. One of the ME materials with magnetically induced ferroelectric order is particularly interesting due to their strong ME coupling, which is important for the electric control of magnetism or vice versa[3]. There are two types of ME materials with the ferroelectricity driven by the magnetic order: one in which ferroelectricity is caused by a noncollinear (spiral) magnetic ordering and the other in which magnetostriction driven ferroelectricity can be induced by collinear magnetic ordering[4]. As such, the origin of magnetic ordering in these material is especially correlated with the ME performance.

The second type of magnetostriction driven ferroelectricity to date is caused by a collinear up-up-down-down ($\uparrow\uparrow\downarrow\downarrow$) magnetic structure. The different distortion of ferro and antiferro bonds ($\uparrow\uparrow$ and $\uparrow\downarrow$) breaks inversion symmetry and results in ferroelectricity. This phenomenon is firstly found in Ca_3CoMnO_6 [5, 6] and then spreads to some double perovskites R_2CoMnO_6 ($R = Y$ or Rare earth metals)[7, 9]. The special $\uparrow\uparrow\downarrow\downarrow$ magnetic structure has been observed in Ca_3CoMnO_6 below $T_N \approx 13$ K and attributed to the stronger exchange interaction between adjacent metal ions with identical spin (next-nearest-neighbor Co-Co and Mn-Mn) than between adjacent metal ions with opposite spins (nearest-neighbor Co-Mn)[10]. Recently, the ferroelectric $\uparrow\uparrow\downarrow\downarrow$ spin configuration has been detected in double perovskites Lu_2CoMnO_6 with magnetic and ferroelectric transition temperature $T_N \approx 35$ K [7] and Y_2CoMnO_6 with $T_N \approx 80$ K[9], while the origin of $\uparrow\uparrow\downarrow\downarrow$ phase has not yet been researched, although it has been proposed to be the same with that in Ca_3CoMnO_6 [7, 9]. However, as we will see below, the structure of R_2CoMnO_6 is very different from Ca_3CoMnO_6 , especially the next-nearest-neighbor (NNN) Co-Co or Mn-Mn distances are much larger (7.41\AA in Lu_2CoMnO_6 and 7.46\AA in Y_2CoMnO_6) than those of Ca_3CoMnO_6 (5.29\AA). Hence,

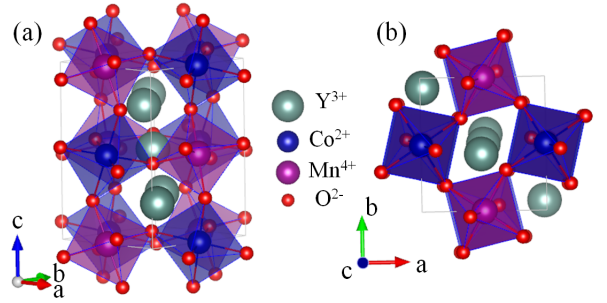


FIG. 1: (color online) Monoclinic structure of Y_2CoMnO_6 . (a) Representation in three dimensions and (b) in the (a,b) plane.

the exchange interactions of NNN Co-Co/Mn-Mn are greatly weakened and not comparable to those of the nearest-neighbor (NN) Co-Mn. Besides, more recently reported magnetic measurements reflect that Y_2CoMnO_6 becomes ferromagnetic below $T_C \approx 75$ K[11]. Therefore, it is highly demanded a further study for Y_2CoMnO_6 to clarify the nature and origin of magnetism, which are crucial for the appearance of ferroelectricity in similar double perovskites.

We performed first-principles calculations to identify the nature and to seek the origin of the magnetic ground state. Our results firstly confirm that the $\uparrow\uparrow\downarrow\downarrow$ state is the magnetic ground state for the $P21/n$ structure determined by experiment. Furthermore, by analyzing the exchange coupling and corresponding pathways, we conclude that the $\uparrow\uparrow\downarrow\downarrow$ spin order in Y_2CoMnO_6 originates from a subtle competition between the ferromagnetic (FM) Co-O-Mn super-exchange and antiferromagnetic (AFM) Co-Mn direct-exchange along c axis. Such subtle magnetic origin, which is very sensitive to even a small perturbation, results in a large discrepancy between theory and experiment results for the polarization of Y_2CoMnO_6 .

Our calculations were performed by using the standard full-potential linearized augmented plane wave code WIEN2k[12]. The muffin-tin sphere radii were chosen to be 2.2, 2.0, 2.0, and 1.4 a.u. for Y, Co, Mn and O atoms, respectively. The cutoff energy of 16 Ry was used for plane wave expansion. The calculations were fully converged using

*Corresponding author: zzen@theory.issp.ac.cn

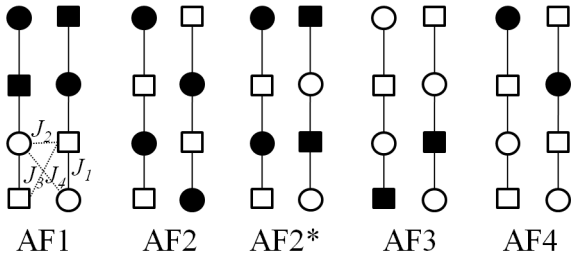


FIG. 2: Schematic representation of magnetic configurations AF1, AF2, AF2*, AF3 and AF4 used in our calculations. Only Co and Mn atoms are drawn: squares and circles denote the Co^{2+} and Mn^{4+} ions, respectively, and the up and down spins are represented by the white and black filling, respectively.

200 k points in the first Brillouin zone. To account for the strong electron correlations, the local spin density approximation plus Hubbard U (LSDA+U) calculations[13] were carried out, with $U = 5$ (4) eV for Co (Mn) and Hund exchange $J = 0.9$ eV for both Co and Mn, which have been widely used in $\text{Ca}_3\text{CoMnO}_6$ [6, 10].

We take the experimental structure data of monoclinic lattice ($P2_1/n$) which have the lattice constant $a = 5.2322\text{\AA}$, $b = 5.5901\text{\AA}$ and $c = 7.4685\text{\AA}$ [9]. As shown in Fig. 1, the MnO_6 and CoO_6 octahedral are corner-sharing and alternate along all a , b , and c directions in double-perovskite Y_2CoMnO_6 . This structural characteristic is obviously different from that of $\text{Ca}_3\text{CoMnO}_6$, in which the MnO_6 and CoO_6 octahedral are face-sharing along c direction and CoMnO_6 chains are isolated by Ca ions. The nearest Co-Mn distance is 3.73\AA in Y_2CoMnO_6 while 2.65\AA in $\text{Ca}_3\text{CoMnO}_6$. In the following, we will explore the magnetic ground state of Y_2CoMnO_6 and its origin according to the structural characteristic.

To confirm that the $\uparrow\uparrow\downarrow\downarrow$ state is the magnetic ground state, six possible magnetic configurations are considered (see Fig. 2): FM, AF1 ($\uparrow\uparrow\downarrow\downarrow$ intrachain and FM interchain), AF2 ($\uparrow\downarrow\uparrow\downarrow$ intrachain and AFM interchain), AF2* ($\uparrow\downarrow\uparrow\downarrow$ intrachain and FM interchain), AF3 ($\uparrow\uparrow\uparrow\downarrow$ with identical spins at the Mn sites), AF4 ($\downarrow\uparrow\uparrow\uparrow$ with identical spins at the Co sites). These states are constructed using $1 \times 1 \times 2$ supercell. From Table I, our LSDA+U results exhibit that the AF1 of $\uparrow\uparrow\downarrow\downarrow$ state is the lowest-energy state, which is consistent with the experimental result from Sharma *et al.*[9]. In addition, the FM and AF2* of $\uparrow\downarrow\uparrow\downarrow$ states, which have been the controversial ground state of Y_2CoMnO_6 [11] and $\text{Ca}_3\text{CoMnO}_6$ [6, 10], are only 10 and 25 meV/f.u. less stable than the ground state AF1. The small energy difference of these three states indicates a weak exchange interaction.

Now, we estimate the exchange constants between magnetic atoms: the NN Co-Mn J_1 , the NNN Co-Mn J_2 , the NN Co-Co J_3 , and the NN Mn-Mn J_4 (Fig. 2(AF1)). By mapping the obtained total energies for each magnetic state to the Heisenberg model, the exchange interactions J_1 , J_2 , J_3 and J_4 were calculated within the approximation:

$$4S^2(4J_1 + 4 \times 2J_3 + 4 \times 2J_4) = E(\text{FM}) - E(\text{AF1}) \quad (1)$$

$$4S^2(8J_1 + 4 \times 4J_2) = E(\text{FM}) - E(\text{AF2}) \quad (2)$$

TABLE I: The total energy E (meV/ (4f. u.)), magnetic moment M (μ_B) per Co/Mn in different magnetic states.

Configuration	E	$M(\text{Co/Mn})$
FM	38	2.57/2.92
AF1	0	2.57/2.89
AF2	290	2.61/2.67
AF2*	100	2.57/2.86
AF3	154	2.59/2.80
AF4	148	2.59/2.77

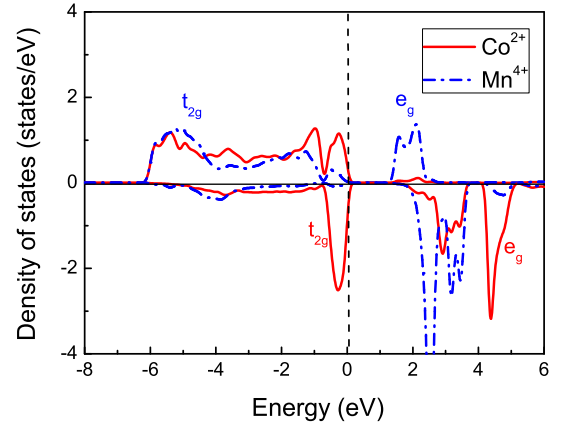


FIG. 3: (color online) The density of states (DOS) of Co-3d and Mn-3d orbitals for the AF1 ground state of Y_2CoMnO_6 by LSDA+U.

$$4S^2(4J_1 + 4 \times 2J_2 + 4 \times 2J_3) = E(\text{FM}) - E(\text{AF3}) \quad (3)$$

$$4S^2(4J_1 + 4 \times 2J_2 + 4 \times 2J_4) = E(\text{FM}) - E(\text{AF4}) \quad (4)$$

Since the spin size of Co^{2+} and Mn^{4+} are stable and are high-spin (see Table I), with the moment $S=3/2$, we get $J_1=0.99$ meV, $J_2=-4.5$ meV, $J_3=0.14$ meV and $J_4=0.22$ meV. These values reflect that in addition to a relatively strong FM interaction along J_2 , all the J_1 , J_3 and J_4 are weakly AF.

Next, the orbital occupations are analyzed to seek the origin of the exchange constant and the ground state. The density of states (DOS) of Co-3d and Mn-3d orbitals for the AF1 ground state are presented in Fig. 3. Y_2CoMnO_6 is insulating with a band gap of 1.2 eV. In the approximately octahedral crystal field, the 3d manifold splits into lower t_{2g} and upper e_g states. For the 3d orbital of Co^{2+} , the up-spin is fully occupied and down-spin is partially occupied on t_{2g} states, which suggests a high-spin Co^{2+} . Mn^{4+} is also high-spin, that is, the three electrons are parallelly occupied on the up-spin t_{2g} states. According to the occupations, schematic energy level and possible interactions are demonstrated in Fig. 4. Along J_1 and J_2 directions, there could be a FM superexchange (SE) via a hopping of Co^{2+} e_g electrons to the empty Mn^{4+} e_g states, and a AFM direct-exchange (DE) between the partially occupied Co^{2+} t_{2g} states and the half occupied Mn^{4+} t_{2g} states. So there is a competition between the FM and AFM couplings. As we know, the SE is more influenced by the Co-O-Mn angle, while the DE is by the Co-Mn distance. Here, the Co-O-Mn angle along J_1 and J_2 are similar, but the Co-Mn

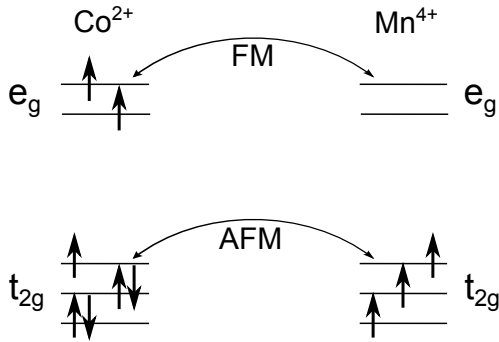


FIG. 4: Schematic crystal field level diagrams of the high-spin Co^{2+} and Mn^{4+} . The e_g electrons hopping leads to a FM coupling while the t_{2g} electrons hopping to a AFM coupling.

distance along J_1 (3.73 Å) is smaller than that along J_2 (3.83 Å). Therefore, the FM SE in both directions are identical and the AFM DE along J_1 could more or less larger than that along J_2 . As a result, a relatively strong FM interaction along J_2 is obtained due to the dominate FM SE, while a strong competition between the FM SE and AFM DE results in a weak AFM interaction along J_1 . As for J_3 and J_4 , only AFM DE exists along both directions. Since the nearest-neighbor Co-Co and Mn-Mn distances (5.34 Å and 5.35 Å) are relatively large, both J_3 and J_4 are weakly AF. All in all, $\uparrow\uparrow\downarrow$ ground state originates from the strong competition between the FM SE and AFM DE along J_1 , like a frustration. As the lowered temperature, the system chooses a crystal distortion or a Co-Mn dimerization to release the competition (frustration), because a definite AFM DE is dominant between the shortened Co-Mn sites while a FM interaction should be the case between the elongated Co-Mn sites.

This picture can be strengthened by the behavior in its sister double perovskites, typically in $\text{Lu}_2\text{CoMnO}_6$ and $\text{La}_2\text{CoMnO}_6$. In $\text{Lu}_2\text{CoMnO}_6$, the Co-O-Mn angle (141.8°) and Co-Mn distance (3.71 Å) along J_1 are very similar with that of Y_2CoMnO_6 (141.6° and 3.73 Å). The above mentioned competition is active and results in the same $\uparrow\uparrow\downarrow$ ground state and hence ferroelectricity in $\text{Lu}_2\text{CoMnO}_6$. However, in another double perovskite $\text{La}_2\text{CoMnO}_6$, a FM ground state with a higher Curie temperature T_c of 226 K has been obtained[14]. The Co-O-Mn angle (157.0°) and Co-Mn distance (3.89 Å) along J_1 are much increased in $\text{La}_2\text{CoMnO}_6$, due to the relatively larger ionic radii of La^{3+} than Y^{3+} and Lu^{3+} . The Co-O-Mn angle close to 180° should enhance the FM SE and the increased Co-Mn distance will weaken the AFM DE. Finally, the competition mentioned before is absent

here and a definite FM ground state is the case.

To see whether there is a Co-Mn dimerization, the structure of Y_2CoMnO_6 in $\uparrow\uparrow\downarrow$ configuration is optimized by relaxing the atom positions but fixing the cell parameters. The optimized structure shows that the Co-Mn distance is 3.75 Å between the two sites with identical spins, and 3.73 Å between that with opposite spins. These atom displacements result in a non-centrosymmetric structure, which is the microscopic source of ferroelectricity in otherwise centrosymmetric structure of Y_2CoMnO_6 . Further to estimate the ferroelectric polarization of Y_2CoMnO_6 , the electric polarizations for the "ferroelectric" optimized structure and "paraelectric" centrosymmetric structure are calculated using the Berry phase method[15]. From the difference of the two structures in polarization, the ferroelectric polarization of Y_2CoMnO_6 is estimated to be 500000 $\mu\text{C}/\text{m}^2$, which is much larger than the experimental value of 65 $\mu\text{C}/\text{m}^2$. This large discrepancy between theory and experiment results for the polarization of Y_2CoMnO_6 is compatible with the subtle magnetic origin, which is very sensitive to even a small perturbation and thus a stable long-range $\uparrow\uparrow\downarrow$ state is difficult to achieve.

To summarize, using first-principles calculations, we find that $\uparrow\uparrow\downarrow$ magnetic structure is the ground state of Y_2CoMnO_6 . From the orbital occupations, both the Co^{2+} and Mn^{4+} are in the high-spin state. Furthermore, the exchange coupling and corresponding pathways are analyzed to seek the magnetic origin, in which the $\uparrow\uparrow\downarrow$ spin order in Y_2CoMnO_6 is found to be originated from a subtle competition between the ferromagnetic Co-O-Mn super-exchange and antiferromagnetic Co-Mn direct-exchange along c axis. At last, our results predict a strong electric polarization of Y_2CoMnO_6 , much larger than the experimental one. This discrepancy most probably arises from that the experiment can not practically achieve the stable long-range $\uparrow\uparrow\downarrow$ state yet. Our derived physical mechanism above will certainly stimulate the on-going experiment.

The author Ting Jia thanks Hua Wu for helpful discussions. This work was supported by the NSF of China (Grant No. 11204309, U1230202), Anhui Province (Grant No. 1308085QA04), the special Funds for Major State Basic Research Project of China (973) under Grant No. 2012CB933702, Hefei Center for Physical Science and Technology under Grant No. 2012FXZY004, and the Director Grants of Hefei Institutes of Physical Science, Chinese Academy of Science (CAS). The calculations were performed in Center for Computational Science of CASHIPS and on the ScGrid of Supercomputing Center, Computer Network Information Center of CAS.

- [1] S.-W. Cheong and M. Mostovoy, Nat. Mater. **6**, 13 (2007).
 [2] R. Ramesh and N. A. Spaldin, Nat. Mater. **6**, 21 (2007).
 [3] W. Eerenstein, N. D. Mathur and J. F. Scott, Nature (London) **442**, 759 (2006).
 [4] D. Khomskii, Physics **2**, 20 (2009).
 [5] Y. J. Choi, H. T. Yi, S. Lee, Q. Huang, V. Kiryukhin, and S. W.

- Cheong, Phys. Rev. Lett. **100**, 047601 (2008).
 [6] H. Wu, T. Burnus, Z. Hu, C. Martin, A. Maignan, J. C. Cezar, A. Tanaka, N. B. Brookes, D. I. Khomskii, and L. H. Tjeng, Phys. Rev. Lett. **102**, 026404 (2009).
 [7] S. Yanez-Vilar, E. D. Mun, V. S. Zapf, B. G. Ueland, J. S. Gardner, J. D. Thompson, J. Singleton, M. Sanchez-Andujar, J.

- Mira, N. Bishop, M. A. Senaris-Rodriguez, and C. D. Batista, Phys. Rev. B **84**, 134427 (2011).
- [8] T. Chatterji, B. Frick and H. S. Nair, J. Phys.: Condens. Matter **24**, 266005 (2012).
- [9] G. Sharma, J. Saha, S. D. Kaushik, V. Siruguri, and S. Patnaik, Appl. Phys. Lett. **103**, 012903 (2013).
- [10] Y. Zhang, H. J. Xiang, and M.-H. Whangbo, Phys. Rev. B **79**, 054432 (2009).
- [11] Chao Zhang, Xiaofei Wang, Haitao Yan, Dawei Kang, Liben Li, Xiaomei Lu, Daofu Han, Feng Yan, Jinsong Zhu, Journal of Electronic Materials **43**, 1071 (2014).
- [12] P. Blaha, K. Schwarz, G. Madsen, D. Kvasnicka, and J. Luitz, Wien2k package, <http://www.wien2k.at>.
- [13] V. I. Anisimov, I. V. Solovyev, M. A. Korotin, M. T. Czyżyk and G. A. Sawatzky, Phys. Rev. B **48**, 16929 (1993).
- [14] R. I. Dass and J. B. Goodenough, Phys. Rev. B **67**, 014401 (2003).
- [15] S.J. Ahmed, J. Kivinen, B. Zaporzan, L. Curiel, S. Pichardo, O. Rubel, Comp. Phys. Commun. **184**, 647 (2013).